Final Report:

CALIBRATION OF ROCK OVERTURNING PROBABILITIES FOR CYBERSHAKE WAVEFORMS

PIs: Glenn Biasi and John G. Anderson

University of Nevada, Reno
SCEC Proposal #13135

Introduction

Purvance et al. (2008) used random vibration theory (RVT) (Boore, 1983) to generate waveforms for development of toppling probabilities of precariously balanced rocks (PBRs) given ground motion parameters PGA, PGV, and SA(1). RVT is an efficient approach to develop large numbers of waveforms for simulation applications where direct computation would be impractical. RVT, however, does not retain the phase relationships among waveform components, and randomness in phasing might affect PBR survival. The SCEC CyberShake project is calculating waveforms at multiple PBR sites that do retain amplitude and phase relationships. This project uses CyberShake waveforms from the San Andreas fault (SAF) source (WGCEP, 2008) to examine toppling probabilities for an ensemble of waveforms computed at the LBUT2 (Lovejoy Buttes) and BKBU (Black Butte) PBR sites near the San Andreas fault. As an infrastructure task we also proposed to estimate pedestal heights for PBRs in the archive as a proxy for PBR age.

CyberShake Waveform Selection and Analysis

Waveforms used here were generated by the CyberShake project using the CVM-SCEC (CVM-S) 3D seismic velocity model under Study 1.4 and provided to us by the CyberShake computational team. Although not the most current version of CyberShake, Study 1.4 is the most recent version for which high-frequency extensions have been calculated. High frequency extensions to the calculated broadband motions are required for this project because while PBRs are most sensitive to ground motions near 1 Hz, higher frequency motions often actually initiate rocking (e.g., DeJong, 2012). Information about CVM-S is available at http://scec.usc.edu/scecpedia/CVM-S. Information on extending CyberShake to high frequencies is available at http://scec.usc.edu/scecpedia/High_Frequency_CyberShake. CyberShake waveforms are provided as velocities in cm/sec, and available only for horizontal components.

A sampling strategy was employed to select waveforms from the CyberShake ensemble. Sampling was necessary because the full set of waveforms was too large for practical management. For example, there are roughly 231,000 waveform variants for the San Andreas source to the Lovejoy Butte site LBUT2. A crafted sampling program was devised. Bands in PGA were defined by $0.1*N<=PGA<0.1*(N+1)$, with N=1,2, …, 9, then sampled at random from that within the subset with a goal of 100 waveforms. This strategy ensures roughly equal population across the ground motion intensity range. A minimum of PGA>0.1 was applied because we know that if accelerations are too small to start the rock vibrating, they cannot topple it. For LBUT2 sampling yielded 645 waveforms.

Table 1. LBUT2 waveform PGA bins and numbers of waveforms sampled.

PGA	#	PGA	#
0.1<=PGA<0.2	100	0.6<=PGA<0.7	81
0.2<=PGA<0.3	100	0.7<=PGA<0.8	30
0.3<=PGA<0.4	100	0.8<=PGA<0.9	20
0.4<=PGA<0.5	100	0.9<=PGA<1.0	14
0.5<=PGA<0.6	100		

The length and source parameters vary from rupture to rupture, but as a group come from the WGCEP (2008) SAF description. Rupture probabilities were not used. Figure 1 shows waveforms for the six 1857-like ruptures in the sample. Figure 2 shows corresponding spectral accelerations (SA). Results here are shown in PGA-SA(1-Hz) axes.

Rock responses to CyberShake accelerograms were estimated using a Matlab version of program *rocking.f*. This program solves for rock rotational response to ground accelerations using a 4th order Runge-Kutta algorithm. For individual waveforms, it indicates whether the rock topples or not given the rock slenderness angle *alpha* and the rocking arm length *R*. In order to leverage the information gained from each CyberShake waveform, all are passed through *rocking* multiple times with increasing scaled values from 0.3 to 2.0 times the computed ground motion. For most waveforms, the rock survives at the lowest scaling, and topples at some point as the input is scaled up. Thus for each waveform, for some ground motion level there is a transition to toppling (Figure 3, green to red symbols; *alpha=0.3* radians, *R*=60 cm, 3.4:1 height:width ratio), along with corresponding PGA and SA(1) values. Results are plotted for individual PGA bands (Table 1). PGA and SA(1) scale linearly, so scaled values plot on a line through the origin with slope SA(1)/PGA.

The spatial ratio of red to green symbols in Figure 3 is a measure of the probability of rock survival at that SA/PGA location under the assumption that waveforms in the PGA range are interchangeable. We calculate this ratio on an overlapping grid in SA-PGA space, and contour the toppling probabilities by location (Figure 4). The blank areas of the upper left and lower right corners show regions of SA-PGA space not developed in CyberShake waveforms. Contours where waveforms do sample give a basis for comparison to previous results. Comparison of North and East component results (Figure 4 upper, lower) suggest that rock response to CyberShake waveforms are generally similar, but that E-W component waveforms are slightly more effective in rock toppling at PGAs near 350 cm/sec^2.

Review of this and other CyberShake waveforms sampled in this study does not suggest that there is anything fundamentally different about CyberShake waveforms when measured by predicted rock survival of accelerogram inputs. However, by its scope this is necessarily an exploratory study, and are continuing to evaluate whether other relationships or views of the data might improve ground motion or waveform shape constraints for use in CyberShake

Pedestal Heights: One task of this project was to estimate PBR pedestal heights for rocks of the PBR archive. Pedestal height is an accessible proxy for the time the PBR has been above the ground surface and thus susceptible to toppling by strong ground motions (Brune et al., 2012). Heights were estimated for 726 rocks (Figure 5). Of these 389 are 50 cm or taller. In Figure 6 we compare rock survival versus distance to the San Andreas fault for all reviewed estimates, and for the subset with pedestal heights greater than 50 cm. The subset exhibits a much more consistent relationship between fragility and distance that also closely parallels median ground motion predictions from Abrahamson and Silva (2008) (Biasi et al., 2014).

References

Abrahamson, N. and W. Silva (2008). Summary of the Abrahamson and Silva NGA ground motion relations. *Earthquake Spectra*, 24(S1), 67-97.

Biasi, G. P., J. N. Brune, and J. G. Anderson (2014). Hazard curve results and a UCERF3-San Jacinto fault comparison from precarious rocks in southern California, *Southern California Earthquake Center Annual Meeting 2014 Proceedings Volume XXIII, September 2014,* poster 067.

Boore, D. M. (1983). Stochastic simulation of high-frequency ground motions based on seismological models of the radiated spectra, *Bulletin of the Seismological Society of America, 73,* 1865-1894.

Brune, R. J., L. Grant-Ludwig, K. Kendrick, and J. N. Brune (2012). Geomorphic erosional models for estimating ages of precariously balanced rocks from cosmogenic isotope data, *Southern California Earthquake Center 2012 Annual Meeting Proceedings Volume,* p.93.

DeJong, M. J. (2012). Amplification of rocking due to horizontal ground motion, *Earthquake Spectra, 28*, 1405-1421.

Working Group of California Earthquake Probability (2007). The Uniform California Earthquake Rupture Forecast, v2, *USGS Open File Report 2007-1437*.

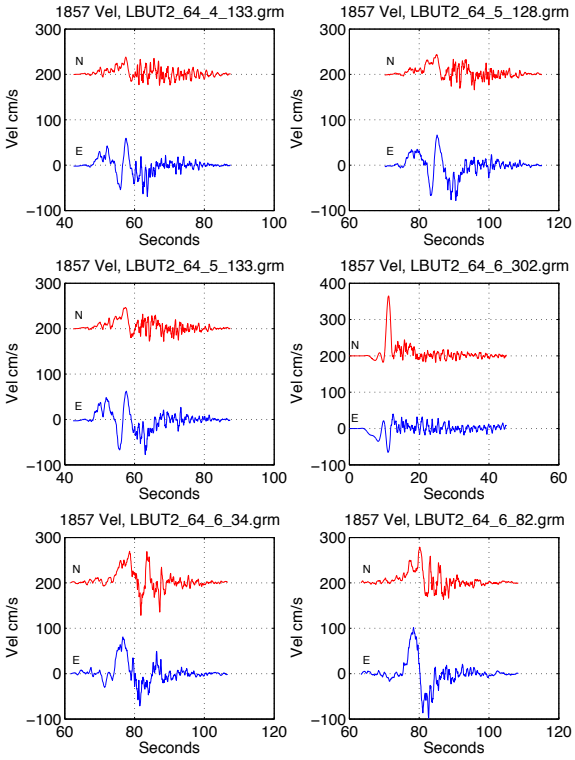

Figure 1. Six waveforms from the southern San Andreas fault source from Cholame to the southern Mojave section (UCERF2 source number 64). This source approximates the 1857 rupture in length and location. Stress drops and directivity contribute to the large ground motion amplitudes in the sample drawn at random.

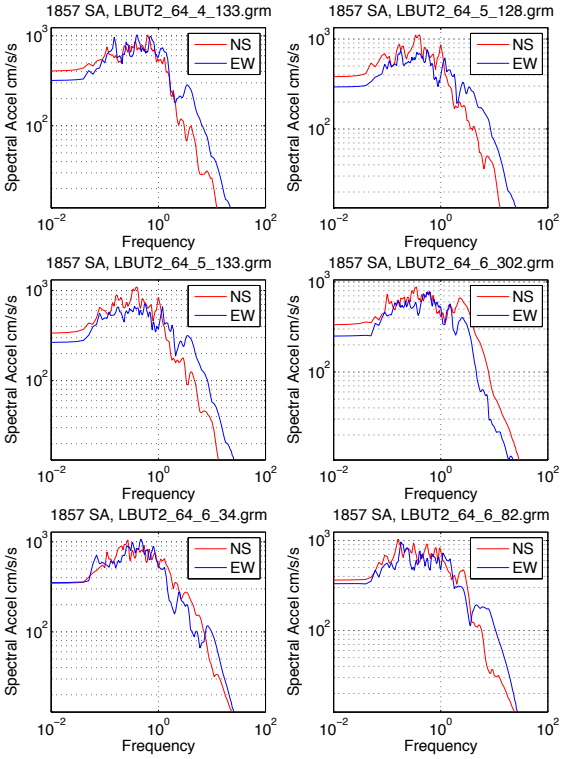

Figure 2: Spectral acceleration for 1857-type sources in Figure 1. Peak SA values reach 1 g for several component motions, and SA at 1 Hz exceeds 0.5 g

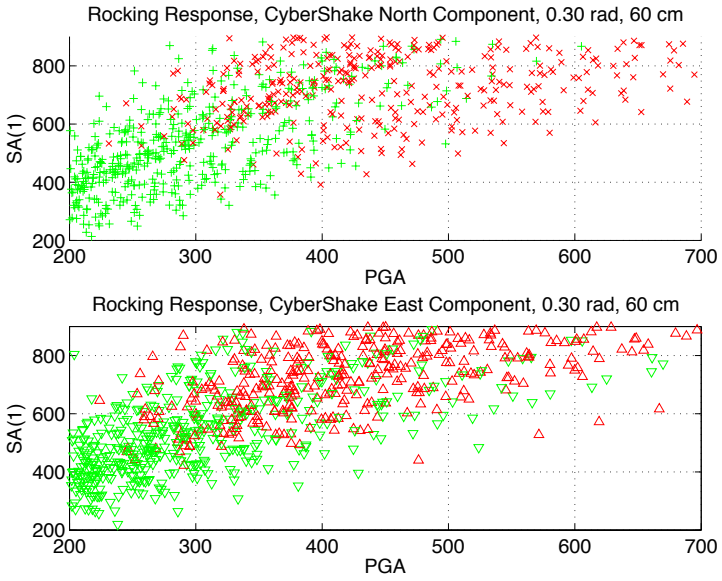

Figure 3. Transitions from survival to toppling for 100 CyberShake waveforms each of north (upper plot) and east components (lower plot) at LBUT2. Green symbols: rock survives at that PGA-SA(1) level. PGA and SA(1) are in cm/sec^2. Slenderness angle is 0.30 radians; rocking arm length is 60 cm. Similar plots were developed for several waveform PGA bins, rocking arm lengths, and alphas.

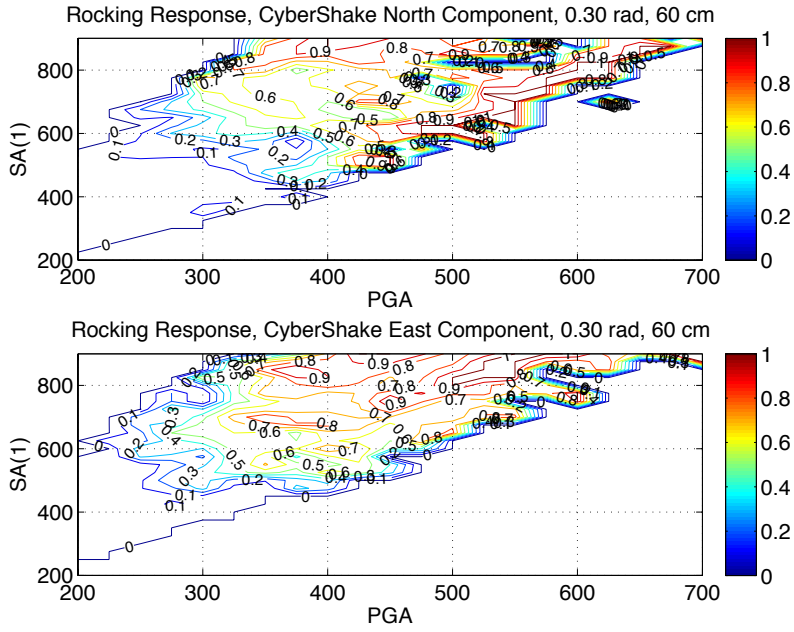

Figure 4. Contoured ratio of survival and toppling for the data in Figure 3. Each point computes the ratio of toppling to surviving values within 25cm/s^2 radius around a given SA-PGA point. Sharp edges of probability to the upper left and lower right corners are artifacts of the lack of waveforms with these SA-PGA pairings.

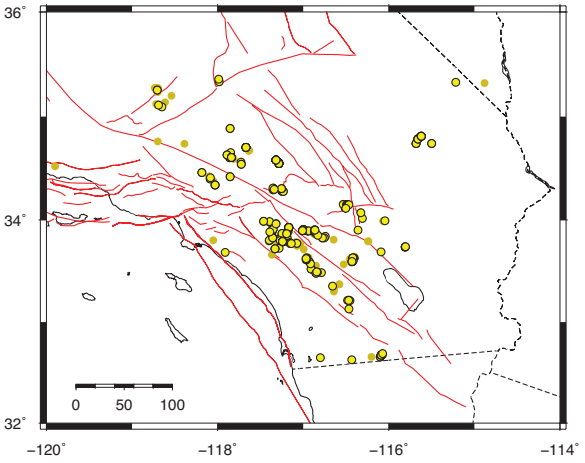

Figure 5. Part of this project was to develop pedestal height estimates for PBRs. Pedestal height is an accessible proxy that scales with rock age (Brune et al., 2012). Dots are PBRs with useable alpha measurements. Circled dots show the subset of new measurements where pedestal heights are greater than 50 cm.

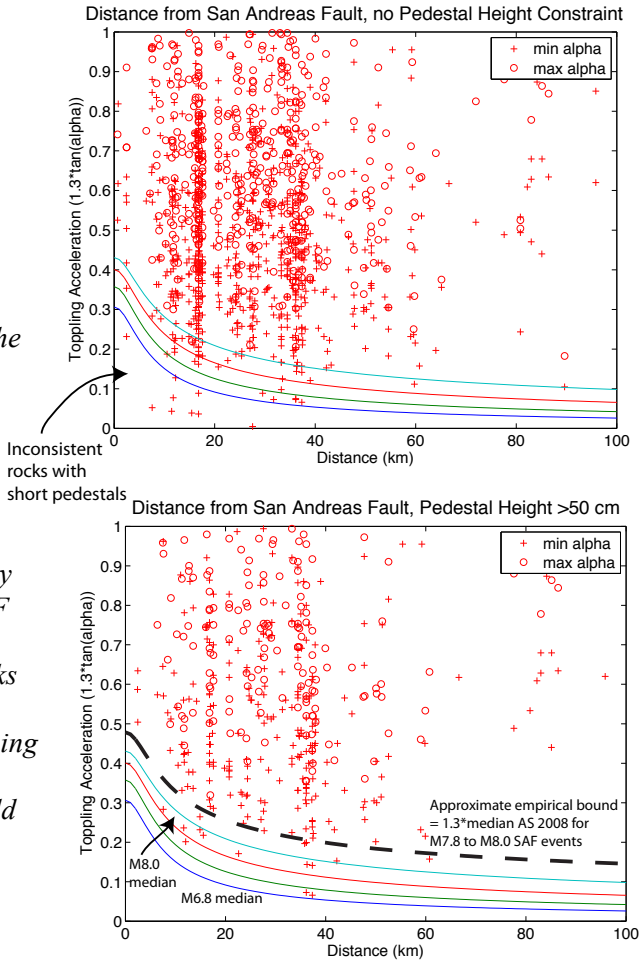

Figure 6. (Upper) Approximate dynamic overturning acceleration for all rocks with reviewed alpha estimates plotted versus distance from the San Andreas fault. "+" is the smaller alpha angle for each rock. Colored lines are from Abrahamson and Silva (2008) median ground motions for Vs 760 m/s site conditions for M6.8, 7.2, 7.6, and 8.0. (Lower) Reviewed estimates for subset of rocks with pedestal heights > 50 cm. Heavy dashed line is an empirical bound suggested by PBR survival of about 1.3x the median for SAF events like what occurred in 1857. Pedestal height is a proxy age filter that eliminates rocks that apparently became precarious recently, perhaps by sudden erosion events. The remaining fraction are consistent with median ground motions expected nearby on the SAF, but would not be consistent with more than about 1 standard deviation above the median.